Advanced Physical Research
Vol.7, No.3, 2025, pp.225-240
https://doi.org/10.62476/apr.73225

NATURAL RADIOACTIVITY AND ASSOCIATED RADDIOLOGICAL HAZARDS IN IMPORTED DECORATIVE BUILDING MATERIALS AVAILABLE IN Al-DIWANIYAH MARKETS, IRAQ

O.N. Oudah

Department of Physics, College of Education, University of Al-Qadisiyah, Iraq

Abstract. In response to the documented rise in cancer cases in Al-Diwaniyah City, this study assesses the specific activities of uranium-238 (^{238}U), thorium-232 (^{232}Th), and potassium- 40 (^{40}K) in commonly used decorative building materials, and evaluates their associated radiological hazards. Twelve imported materials were selected based on popularity and indoor usage, where prolonged human exposure is likely. Gamma spectrometry with a $3'' \times 3''$NaI(TI) detector was employed for activity measurements. The activity measurements ranged from 4.20 ± 0.49 to 34.81 ± 1.45 Bq/kg for ^{238}U, 3.09 ± 0.92 to 73.33 ± 1.33 Bq/kg for ^{232}Th, and 196.09 ± 0.09 to 1787.79 ± 3.66 Bq/kg for ^{40}K, with ^{40}K showing the highest levels. Calculated hazard indices included radium equivalent activity Ra_{eq} (37.89 – 243.52 Bq/kg), absorbed dose rate DR (18.36 – 119.63nGy/h), annual effective dose equivalent AEDE (0.01 – 0.58mSv/y), and activity utilization index AUI (0.18-1.06). While most indices were within safety limits, excess lifetime cancer risk ELCR values $\left(0.31 \times 10^{-3} - 2.03 \times 10^{-3}\right)$ exceeded international thresholds in some samples. A significant correlation was observed between ^{232}Th and ^{40}K. Although average values complied with UNSCEAR recommendations, certain samples presented potential health risks, underscoring the need for stricter monitoring and regulatory control of imported decorative materials used indoors.

Keywords: Radiological Hazards, Gamma-ray spectroscopy, Decorative Building Materials, Activity utilization index, UNSCEAR.

Corresponding author: O.N. Oudah, Department of Physics, College of Education, University of Al-Qadisiyah, Iraq, e-mail: *osamah.oudah@qu.edu.iq*

Received: 8 July 2025; Revised: 1 August 2025; Accepted: 23 August 2025; Published: 16 October 2025.

1 Introduction

The raw building materials naturally contain radioactive elements such as ^{238}U, ^{232}Th, and ^{40}K Baha et al. (2023), these natural radionuclides are present in all materials used in construction, finishing, and decoration, like gypsum, tiles, granite, marble, etc. The natural radioactivity varied depending on geographic and geological circumstances. It exists in the soil at various levels in each area around the world Salman et al. (2024). In general, most people spend their time indoors, therefore, they will be exposed to larger doses of radiation, and these materials may cause a large dose of gamma rays (ICRP, 2011). It is worth mentioning that the effect of radiation on humans appears in the form of diseases or genetic changes depending upon the dose received and the exposure interval (Ali et al., 2020).

Cancer incidence in Iraq has shown a significant upward trend, with new cases reaching around 39,068 in 2022 (Ministry, 2022). In Al-Qadisiyah Governorate, 1,290 cases were reported in 2022, including 537 males (41.6%) and 753 females (58.4%). The number of cases in this region rose steadily over the past three years, from 1,101 in 2020 to 1,290 in 2022, with the incidence rate rising from 81.01 to 90.2, according to the Iraqi Cancer Registry (Ministry, 2022), so the estimation of the specific activity for radionuclides is important to know the levels of radiation for decorative materials to assess the radiation hazards that may affect human health as well as the necessity of establishing standards and guidelines on how these materials are used and managed, secondly, the knowledge of radioactivity is necessary for companies and people who construct buildings to take into account the necessary precautionary measures to prevent the effects of radiation. Several studies have assessed natural radioactivity levels in building and decorative materials across Iraq and other countries. In Iraq, Abdellah et al. reported that most studied materials are safe, with average concentrations of ^{326}Ra,^{232}Th, and ^{40}K being $35.26, 26.99$, and 321.19 Bq/kg, respectively, while decorative materials showed higher risks (Abdellah et al., 2018). Jassim and Abojassim confirmed that decorative stones had the highest specific activities of ^{238}U,^{232}Th, and ^{40}K (Jassim et al., 2022). In Erbil, Othman et al. observed wide variations, particularly in granite samples (Othman et al., 2023). Ali found that concentrations of ^{226}Ra reach 223.7 Bq/kg (Ali, 2012). Amana noted that ceramic tiles exceeded global averages for ^{238}U and ^{232}Th, while ^{40}K remained within safe limits (Amana, 2017). In Karbala, Omron and Salim measured the highest values in imported granite and marble samples, though still below UNSCEAR limits (Omron & Salim, 2020). Dawal and Oudah assessed natural radioactivity in bricks from Babylon, Iraq. The average concentrations were $18, 41.7$, and 352.4 Bq/kg. All values were within permissible limits except for ^{232}Th, which exceeded recommended levels in some samples (Dawal & Oudah, 2025).

Internationally, Al-Sewaidan found elevated activities in Saudi ceramic materials, especially for ^{40}K (up to 1269 Bq/kg) (Al-Sewaidan, 2019). In Egypt, Hassan et al. identified granite as having extremely high radionuclide levels, reaching 78.75 kBq/kg for ^{226}Ra (Hassan et al., 2013). In Turkey, Turhan et al reported that clay bricks and granite had the highest radioactivity among 15 material types Turhan et al. (2022). Joel et al. in Nigeria measured average values of $61.1, 70.2$, and 514.7 Bq/kg for ^{226}Ra, ^{232}Th, and ^{40}K in commercial tiles, respectively (Joel et al., 2018). Further studies have also highlighted radiological assessments in building materials from other regions. Omogunloye et al. analyzed five categories of materials commonly used in Pietermaritzburg, South Africa, reporting that while ^{40}K remained within global safety limits, both ^{238}U and ^{232}Th exceeded international averages Omogunloye et al. (2025). In Nigeria, Gambo et al. investigated 19 materials used in Katsina State. They found that, although some materials such as gravel and clay exceeded the average values for ^{238}U and ^{40}K, all measured concentrations remained below the global upper limit, indicating no significant radiological hazard in their use for construction (Gambo et al., 2025).

Although cancer rates have increased in Al-Qadisiyah Governorate over the past decade (Ministry, 2022), this study does not attempt to directly link the elevated radionuclide levels in decorative materials to the regional cancer incidence. Rather, our results underscore the importance of evaluating radiological risks in indoor environments. Prior studies (e.g., (Wakeford, 2004; Zlobina et al., 2022)) have noted that long-term exposure to elevated natural gamma radiation may contribute to increased cancer risk, which highlights the importance of regulatory oversight and informed material selection in the construction sector, and environmental concern that warrants further epidemiological investigation. Several investigations have identified noticeable concentrations of radionuclides in construction materials. Still, no comprehensive assessment has been conducted on the materials used in Al-Diwaniyah. This absence of data represents a significant research gap that this study aims to address by investigate the activity levels of ^{238}U, ^{232}Th, and 40K, predict the relationship between them in nature through appropriate statistical methods, and assess potential radiation risks associated with decorative materials collected from various local markets in Al-Diwaniyah city to provide specialists, researchers, decision-makers, and others interested in the health sector with comprehensive information on the levels of radioactivity and associated risks resulting from using finishing building materials that are in direct contact with users.

2 Materials and Methods

2.1 Sample Collection and Preparation

The samples were selected from local markets in Al-Diwaniyah city (center of Al-Qadisiyah Governorate), based on their widespread use among consumers and their affordability, which makes them accessible to a broader segment of the population. Through interviews conducted with several local vendors of finishing and decorative materials, the study identified twelve of the most commonly traded decorative building materials. These are listed in Table (1). Sample processing took place in the Radiation Laboratory within the Physics Department at the University of Kufa. All samples were ground using a specialized mill and converted into fine powder, and subjected to thermal treatment at 110^{o}C for approximately one hour to ensure the removal of residual moisture. Subsequently, they were passed through a $300\mu m$ mesh to achieve uniformity, with the final mass reaching around 750 grams. The beakers were sealed with tape. To achieve secular equilibrium for ^{238}U, ^{232}Th, and their progenies, all samples were stored in polyethylene containers for four weeks (Omogunloye et al., 2025; Aswood et al., 2019).

Table 1: The samples of decorative materials used in this study.

Sample code	Local name*	Country
D01	Floor tiles	Iran
D02	Quartz stone	China
D03	Natural granite	China
D04	Mica stone	China
D05	Par Tavoosi marble	Iran
D06	Unker Crane Stone	Iran
D07	Industrial granite	Iran
D08	Cappuccino stone	Iran
D09	Black granite	Iran
D10	Ceramic wall tiles	Turkey
D11	Porcelain	Iran
D12	Trunky stone	Iran

Note: The sample names are translated into English from the local name used by the local population.

2.2 Experimental Procedure

Gamma-ray measurements were performed using a NaI(TI) scintillation detector $3'' \times 3''$ crystal coupled to a 4096-channel multi-channel analyser (MCA) via an analog-to-digital converter, with an energy resolution (FWHM) of 7.9% at the 1.33 MeV peak of ^{60}Co. Background radiation was minimized using an ORTEC cylindrical shield (22 cm diameter) comprising an inner stainless-steel layer (20 cm thick) and an outer lead layer (5 cm thick). The detector was connected to the computer, and the gamma spectrum was recorded via the MAESTRO-32 program.

Detector calibration was carried out for energy and efficiency using certified reference gamma sources (^{137}Cs,^{60} Co, and ^{22}Na; activity $\approx 1\mu$Ci) provided by IAEA. The sources were placed in 1 L Marinelli beakers to match the sample geometry and positioned at the same distance from the detector as the measured samples. Energy efficiency calibration covered the range $500-2500$keV, yielding a calibration curve ($R^2 = 0.999$). The measured efficiencies for the certified sources deviated by less than $\pm 5\%$ from their reference values, confirming the accuracy of the calibration. Quality control was ensured by periodic measurements of standard reference materials and by analysing duplicate samples at regular intervals to verify measurement reproducibility (IAEA, 1989).

Specific activities of ^{238}U and ^{232}Th were determined from the 1764.49keVγ-line of ^{214}Bi (15.96% probability) and the 2614keVγ-line of ^{208}TI (99% probability), respectively, while ^{40}K activity was obtained from the 1460 keV γ-line (11% probability) (Omogunloye et al., 2025;

Aswood et al., 2019). Each sample was counted for 5h to achieve statistically reliable spectra.

3 Calculations

3.1 The specific activity

The specific activity C_n Bq/kg of gamma emissions was calculated by equation (1) (Alhous et al., 2020):

$$C_n = \frac{C}{\varepsilon I_\gamma LTm}, \tag{1}$$

where C_n Bq/kg specific activity, C the net area below peak per second and delete the context from under this value, ε is efficiency, I_γ is the probability of radiation emission, LT counting lifetime measured in (sec) and m the mass of sample (kg).

3.2 Radium Equivalent Activity

This parameter is used to assess the safety of materials and ensure that they do not pose a significant radiation hazard, calculated using equation (2) (Kadhim et al., 2020):

$$R_{aeq} = C_U + C_{Th}C_{Th} + C_K C_K, \tag{2}$$

where: Raeq Radium Equivalent Activity, C_u, C_{Th} and C_K the specific activity (Bq/kg) of $^{238}U, ^{232}Th$, and ^{40}K. CFTh and CFK are the conversion factor for ^{232}Th and ^{40}K, which equal 1.43 and 0.077 respectively (Dawal & Oudah, 2025).

3.3 Dose Rate (DR)

The exposure to the natural radionuclides has a direct connection identified as the (DR) determined by equation (3) (UNSCEAR, 2000):

$$DR = C_U DF_U + C_{Th} DF_{Th} + C_k DF_k \tag{3}$$

Where: DR Dose Rate (nGy/h), DFu, DFTh, and DFk are dose conversion factors for $^{238}U, ^{232}Th$, and ^{40}K, equal to 0.462, 0.604, and 0.0417 respectively (Dawal & Oudah, 2025).

3.4 Annual Effective Dose Equivalent indoor

DR can be used to compute the $AEDE_{indoor}$ (mSv/y) from a formula known by UNSCEAR (UNSCEAR, 2000).

$$AEDE_{indoor} = DR^2 \times No.h \times F \times O \times 10^{-6}, \tag{4}$$

where: AEDE indoor Annual Effective Dose Equivalent indoor, No.h number of hours an individual is exposed to radiation throughout the year (8760 h/y), F is the coefficient of conversion acquired by mature individuals (0.7 Sv/Gy), and O is the occupancy factor for indoor (0.8), 10^{-6} multiplying factor for unit conversion from (nGy) to mSv (UNSCEAR, 2000).

3.5 Internal and External Hazard Indices

Internal and External hazards were determined using equation (5) and (6) (Darwish, 2015):

$$H_{in} = \frac{C_U}{185} + \frac{C_{Th}}{259} + \frac{C_K}{4810} \leq 1 \tag{5}$$

$$H_{ex} = \frac{C_U}{370} + \frac{C_{Th}}{259} + \frac{C_K}{4810} \leq 1, \tag{6}$$

where: H_{in} and H_{ex} Internal and External hazards, the values 185, 259, 370, and 4810 (in Bq/kg) are standard limits for $^{238}U, ^{232}Th$, and ^{40}K to keep the hazard index ≤ 1, corresponding to 1mSv/y (UNSCEAR, 2000).

3.6 Cancer Risks Associated with the Use of Decorative Material

By using equation (4) the $ELCR_{indoor}$ is determined through Eq. (7) (Keser et al., 2011):

$$ELCR_{\text{indoor}} = \text{AEDE}_{\text{indoor}} \times DL \times RF, \tag{7}$$

where: $ELCR$ indoor excess lifetime cancer risk, DL the average lifespan of a human, RF (Sv^{-1}) coefficient of the risk. Average life span is estimated at 70 years; RF for random effects is used as 0.05 Sv^{-1} for the public based on ICRP (Keser et al., 2011).

3.7 Activity Utilization Index

AUI is used to estimate the safety of using a particular building material. It is calculated using the equation (Kumar et al., 2022):

$$\text{AUI} = \frac{c_U}{50} f_U + \frac{c_{Th}}{50} f_{Th} + \frac{c_K}{500} f_k \tag{8}$$

where: AUI Activity Utilization Index, f_U, f_{Th}, and f_k are the respective fractional contributions for three-element which equal (0.462), (0.604) and (0.042) respectively (UNSCEAR, 2008).

4 Results and Discussion

The activity concentrations for ^{238}U were measured to be between 4.20 ± 0.49 and 34.81 ± 1.45 Bq/kg, with an average of 13.09 ± 0.83 Bq/kg, as shown in Table 2. Notably, sample D11 (Iran) exhibited the highest ^{238}U activity among all samples. However, its value remains slightly below the recommended safety limit set by (UNSCEAR, 2000). The findings align with those mentioned by Ahmed et al., who pointed out that the concentrations of ^{238}U in the analyzed samples were generally below the international average (Ahmed, 2005). While the quartz sample in this study Farhan et al. (2022) approached the threshold levels set for radiological safety by UNSCEAR. Similarly, elevated levels were reported in some cases by the study Jassim et al. (2022), although the average is below the global limit. Similar outcomes were documented in references Omron & Salim (2020) and Ali et al. (2025), which also showed low ^{238}U levels in decorative materials, suggesting consistency across results. However, study UNSCEAR (2000) presented a different trend, as it recorded much higher levels of ^{238}U, reaching 174 Bq/kg.

As for the ^{232} Th activity, values ranged between 3.09 ± 0.92 and 73.33 ± 1.33Bq/kg. The average was 29.10 ± 0.82 Bq/kg, as shown in Table 2. Although most values were within the acceptable safety margin set by UNSCEAR, certain samples-especially D03, D04 (China), and D11, D06 (Iran)-recorded elevated values, which may suggest a geological source containing thorium-rich minerals. These findings are consistent with those reported by Al-Zahrani in Saudi Arabia, who documented ^{232}Th concentrations in granite samples ranging between 0.51 and 89.82 Bq/kg, with an average of 34.83 Bq/kg [Al-Zahrani (2017)]. Similarly, Dawal and Oudah recorded a mean value of 47.0 ± 2.8 Bq/kg in brick samples from Babylon (Dawal & Oudah, 2025). Studies conducted in other regions of Iraq also reflect comparable results: Omron and Salim reported an average of 24.97 Bq/kg (Omron & Salim, 2020), and Jafir et al. found a mean of 30.30 Bq/kg (Jafir et al., 2024). In contrast, significantly higher values were reported by Yang and Lin in China, with an average of 106.7 ± 5.2 Bq/kg (Yang & Lin, 2021). Likewise, Ahmed reported a mean of 64 ± 34 Bq/kg in building materials from Egypt, with the highest value (118 ± 14Bq/kg) found in granite samples (Ahmed, 2005).

On the lower end, several studies have documented much lower averages for ^{232}Th, including Taqi et al. in Kirkuk, Iraq (mean 11.84 Bq/kg) Taqi et al. (2018), Imani et al. in Iran (23 ± 4 Bq/kg) (Imani et al., 2021), and Amana et al. in Iraqi cement (15.97 Bq/kg) (Amana et al., 2021). Othman and Hussein similarly recorded a moderate average of 22.95 ± 2.86 Bq/kg in Sulaymaniyah (Othman et al., 2023), while Essa et al. reported one of the lowest averages at

8.00 Bq/kg (Essa et al., 2025). The mean ^{232}Th activity observed in the current study aligns with the global and regional averages, yet the presence of samples with elevated concentrations, particularly those imported from China and Iran, underscores the need for monitoring and regulatory control of such materials before their widespread use in enclosed indoor environments.

The activity concentrations of ^{40}K ranged from 196.09 ± 3.66 to 1787.79 ± 10.73 Bq/kg, with an average of 703.37 ± 6.26 Bq/kg (Table 2). This value represents the highest among the three measured radionuclides, which is expected given the natural abundance of ^{40}K in various silicate-rich rocks. Several samples-particularly D06, D03, D04 (China), D11, and D12 (Iran), as well as D10 (Turkey)-exceeded the global limit of 400 Bq/kg (UNSCEAR, 2000). Comparable or even higher ^{40}K concentrations have been reported in the literature. For example, Yang and Lin measured average values of 1004.2 ± 19.8 Bq/kg in building decoration materials from China (Yang & Lin, 2021), and similarly elevated values were found in both marble and ceramic tiles. Al-Zahrani reported ^{40}K values ranging from 19.47 Bq/kg in Iranian white granite to 1632.37 Bq/kg in Saudi Arabian black-and-red granite, with an overall average of 665.08 Bq/kg (Al-Zahrani, 2017).

Further evidence comes from Pavlidou et al., who observed a wide range of 49 ± 4 to 1592 ± 39 Bq/kg in granite, recording a high average 1104 Bq/kg (Pavlidou et al., 2006). Likewise, Hassan et al. reported concentrations ranging from 32.60 ± 4.25 to 2238.33 ± 242.66 Bq/kg in marble samples, and 1069.83 ± 124.50 Bq/kg in ceramicsboth used extensively in interior finishes (Hassan et al., 2017). Dawal and Oudah found activity levels ranging from 272.2 ± 5.8 to 399.1 ± 7.1 Bq/kg in Iraqi brick materials (Dawal & Oudah, 2025). Imani et al. reported a broader range of elevated levels in granite (7141085 Bq/kg) (Imani et al., 2021). Ahmed recorded 1500 Bq/kg (in marble) (Ahmed, 2005), while Jassim and Abojassim reported a high level of 838.2 ± 8.8 Bq/kg in decorative alabaster (Jassim et al., 2022). Amana et al. found lower values in locally produced Iraqi cement (Amana et al., 2021), and Essa et al. observed similar results in cement as well (Essa et al., 2025).

Overall, the average ^{40}K activity in the current study is relatively high compared to several regional and international reports, and in some cases, approaches or exceeds the upper bounds observed elsewhere. This may be attributed to the mineralogical composition of the imported materials—particularly feldspar- and mica-rich granites and highlights the need for regulatory oversight of such products when intended for indoor application. While the average ^{232}Th activity aligns with global averages, the variability across samples-particularly those from China and Iran-emphasizes the need for regulatory attention toward imported materials of geological origin known for thorium enrichment.

Table 2: Specific activity (Bq/kg) for studied radionuclides.

Sample code	^{238}U		^{232} Th		^{40}K	
	Value	± SE	Value	± SE	Value	± SE
D01	17.62	1.06	3.09	0.92	223.07	4.02
D02	5.7	0.60	14.38	0.61	477.71	5.81
D03	4.2	0.49	73.33	1.33	1605.32	10.28
D04	14.74	0.92	61.25	1.21	1598.7	10.23
D05	12.15	0.83	7.57	0.42	219.72	3.76
D06	9.3	0.73	67.53	1.62	1787.79	10.73
D07	14.12	0.92	6.07	0.39	196.09	3.66
D08	9.52	0.77	15.42	0.63	310.86	4.66
D09	11.43	0.85	8.46	0.47	311.37	4.70
D10	4.11	0.50	8.86	0.47	424.84	5.43
D11	34.81	1.45	43.42	1.03	756.43	7.16
D12	19.38	0.84	39.76	0.77	528.49	4.68
Min	4.2	0.49	3.09	0.92	196.09	3.66
Max	34.81	1.45	73.33	1.33	1787.79	10.73
Mean	13.09	0.83	29.10	0.82	703.37	6.26
Safe limit (UNSCEAR, 2000)	35		30		400	

The standard deviations of the natural radionuclides indicate varying degrees of dispersion among the samples. For example, the SD of ^{238}U was 2.87 Bq/kg (21.9% of the mean), reflecting moderate variability. The observed standard deviation for ^{238}U reflects moderate dispersion across the analyzed samples. Such variability is expected and considered acceptable in natural materials due to inherent geological heterogeneity and differences in mineral composition. This interpretation is consistent with literature stating that standard deviations between 10% and 30% are typical and acceptable in radiological studies of natural building materials (Dos et al., 2021), reported coefficients of variation ranging from 33% to over 50% for Ra_{eq} in ceramic raw materials, attributing the variability to differences in extraction sites, clay quality, and geological heterogeneity of the source materials. Therefore, the moderate dispersion observed in ^{238}U activity is within expected limits for such materials. ^{232} Th showed lower variability (2.84 Bq/kg; 9.8% of the mean), while ^{40}K had a very low SD (21.68 Bq/kg; 3.1% of the mean), suggesting a relatively homogeneous distribution. These differences may be attributed to the diverse lithological and mineralogical origins of the materials analyzed, particularly for imported decorative stones and ceramics.

Notably, the samples with activities exceeding UNSCEAR safety limits (e.g., D03, D04, D06, D11) also correspond to the highest variability values, indicating that elevated activity levels tend to be associated with greater dispersion among replicates and across the dataset.

Table 3 summarizes a comparative overview of the means of the studied radionuclide levels from selected studies conducted inside and outside Iraq, alongside the present study. While the detailed discussion of these references was presented earlier, Table 3 quantitatively demonstrates that the average ^{238}U value is significantly below most previous reports, indicating a reduction of approximately 71% from the average. Similarly, the mean ^{232}Th activity also showed a moderate decrease (about 26%) compared to earlier findings. In contrast, the ^{40}K mean value in the present study was notably higher by nearly 38% than the regional average, highlighting its dominant contribution among the measured radionuclides. These results support the earlier interpretation that the variation in radionuclide activity levels across studies is strongly influenced by the geological origin, mineral content, and industrial processing of the decorative materials.

Table 3: The present study versus other studies.

Position	Mean specific activity (Bq/kg)			Ref
	^{238}U	^{232} Th	^{40}K	
Iraq	25.19	10.97	313.22	(Jassim et al., 2022)
Iraq	91.90	50.4	482.37	(Najam et al., 2023)
Iraq /Karbala	23.92	24.97	207.99	(Omron & Salim, 2020)
Turkey	15.85	33.76	359	(Pavlidou et al., 2006)
Iran	72	76	1193	(Asgharizadeh et al., 2012)
Iraq / Al Diwaniyah	13.09	29.10	703.37	P.S

5 Statistical analyses

5.1 R-squared (coefficient of determination)

The values of R^2 between (^{238} U,^{232}Th) and (^{238} U, ^{40}K) are 0.0035, 0.0141 respectively, indicates the model that explains the relationship does not perfectly explain the variance in the data and has no predictive value, but the R^2 value 0.9019 between ^{232}Th and ^{40}K indicates that the model explains a large amount of the variance in the data and perfectly predicts values in the target field (90% of the variation in the output variables are explained by the input variables). Figures (1-3) and Table 4 below show the R-squared values between the studied elements.

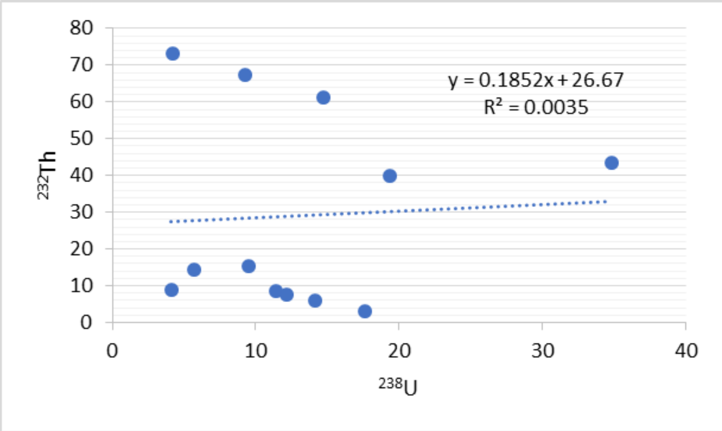

Figure 1: R-squared values for ^{238}U and ^{232}Th..

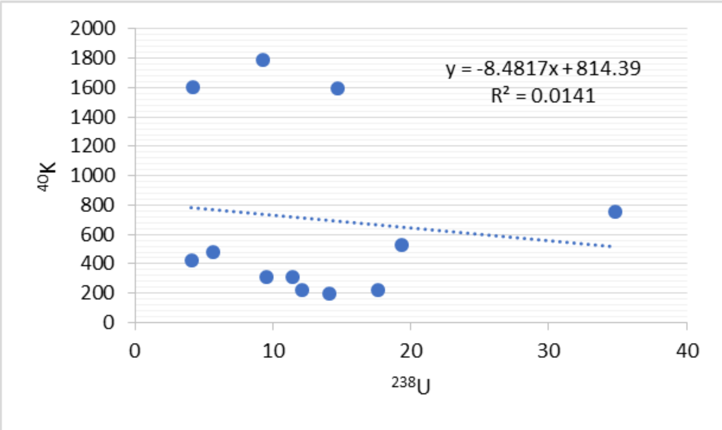

Figure 2: R-squared values for ^{238}U and ^{40}K.

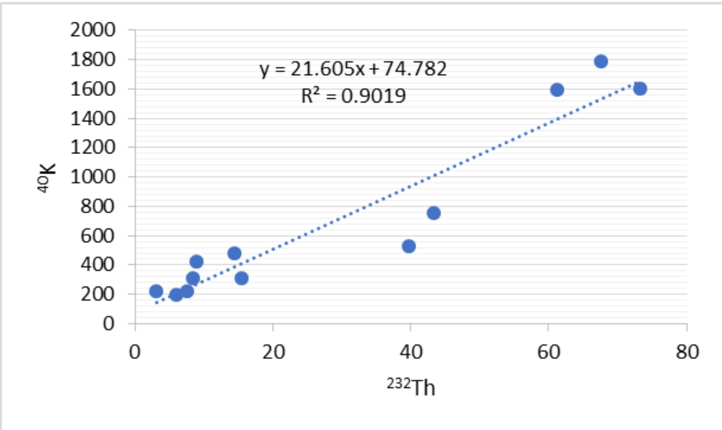

Figure 3: R-squared values for ^{232}Th and ^{40}K.

Table 4: R-squared for studied radionuclide.

	^{238}U	^{232}Th	^{40}K
^{238}U	1	0.0035	0.0141
^{232}Th	0.0035	1	0.9019
^{40}K	0.0141	0.9019	1

5.2 P-value

The probabilities (P-value) for studied radionuclide are listed in Table 5. The results are significant at a probability (P-value) less than 0.05 amongst ^{238}U,^{232} Th, and ^{40}K. The relationship between ^{238}U and ^{232}Th is statistically insignificant also ^{238}U and ^{40}K, but the relationship between ^{232}Th and ^{40}K is statistically significant, which means that the relationship between ^{232}Th and ^{40}K does not obey chance in this case, also helps us to predict the pollution caused by ^{232}Th by measuring ^{40}K specific activity and vice versa.

Table 5: P-values for studied radionuclide.

	^{238}U	^{232}Th	^{40}K
^{238}U	0	0.855483	0.71319
^{232}Th	0.855483	0	2.33×10^{-06}
^{40}K	0.71319	2.33×10^{-06}	0

5.3 Pearson Correlation

Pearson statistics were used to assess the correlation degree between ^{238}U,^{232} Th and ^{40}K, to find out whether the change in one measurement or all measurements is related to the change in measurements in the corresponding group, as illustrated in Table 6. Although there are positive and negative correlations, the relationships between ^{238}U with ^{40}K are weak (Weak negative linear relationship). Also, the relationship between ^{238}U and ^{232}Th is weak despite a positive correlation (positive linear relationship is weak). The relationship between ^{232}Th and ^{40}K has a significant positive correlation as expected at 0.94 it gives a measure of 94% of the probability of one variable increasing when the other variable increases (strong direct correlation).

Table 6: Correlation coefficient for ^{238}U, ^{232}Th, and ^{40}K.

	^{238}U	^{232} Th	^{40}K
^{238}U	1		
^{232}Th	0.058997	1	
^{40}K	-0.11875	0.949673	1

The observed strong positive correlation between ^{232}Th and ^{40}K($r = 0.94$) likely reflects their shared geochemical behavior and frequent co-occurrence in felsic igneous rocks such as granite and syenite. Both ^{232}Th and ^{40}K are incompatible trace elements, meaning they are preferentially concentrated in the residual melt during magmatic differentiation instead of being incorporated into early-crystallizing minerals. This promotes their enrichment in accessory minerals such as K-feldspar, muscovite, biotite, and monazite-especially in evolved granitic rocks (Albarède, 2003; Curtis, 1956; Fall et al., 2020).

At the same time, ^{232}Th has been observed to correlate well with ^{40}K in potassiumrich felsic rocks, where minerals like K-feldspar dominate the assemblage. These correlations arise from the geochemical affinity of ^{232}Th and ^{40}K to residual silicate melts, especially during late stages of crystallization (Abdel-Hakeem et al., 2023; Fall et al., 2020).

This geochemical pattern is further supported by studies of two-mica granites, which are rich in muscovite and biotite. These rocks frequently show elevated levels of both ^{232}Th and ^{40}K, in line with the mineralogical hosts: potassium-bearing minerals (Kfeldspar, muscovite, biotite) and Th-hosting accessory phases (monazite, zircon). Such findings are consistent with the mineralogical and lithological nature of the raw materials in the studied samples, indicating that the correlation between ^{232}Th and ^{40}K is not coincidental, but rather geochemically driven (Gaafar et al., 2014; Fall et al., 2020).

5.4 Multivariate Statistical Analysis

To further explore the underlying patterns among the studied samples and classify them based on their radiological profiles, a Principal Component Analysis (PCA) was performed using the specific activities of ^{238}U,^{232} Th, and ^{40}K. The PCA results revealed that PC1 accounted for 65.05% of the total variance, while PC2 explained an additional 33.82%, making the cumulative explained variance 98.87%. This indicates that the vast majority of variation in radionuclide concentrations can be effectively captured by these two components.

The biplot of PCA (Figure 4) showed clear differentiation among the samples. Samples such as D03, D04, and D06 clustered towards the right along PC1, suggesting high contributions from ^{40}K and ^{232}Th. Conversely, samples like D01, D05, and D07 are positioned to the left, indicating relatively lower radionuclide levels. The samples D11 and D12 appeared in the upper region of the plot, suggesting influence from PC2, likely driven by a distinctive pattern of ^{238}U and ^{232}Th concentrations. These findings suggest the existence of distinct radiological signatures, possibly due to varying geological sources or material origins, consistent with findings reported in similar multivariate studies on building materials (e.g., (Imani et al., 2021)).

Overall, PCA proved to be a valuable tool for visualizing groupings among samples and provided strong statistical support for interpreting potential sources and patterns in radionuclide distribution, beyond what univariate analysis could offer.

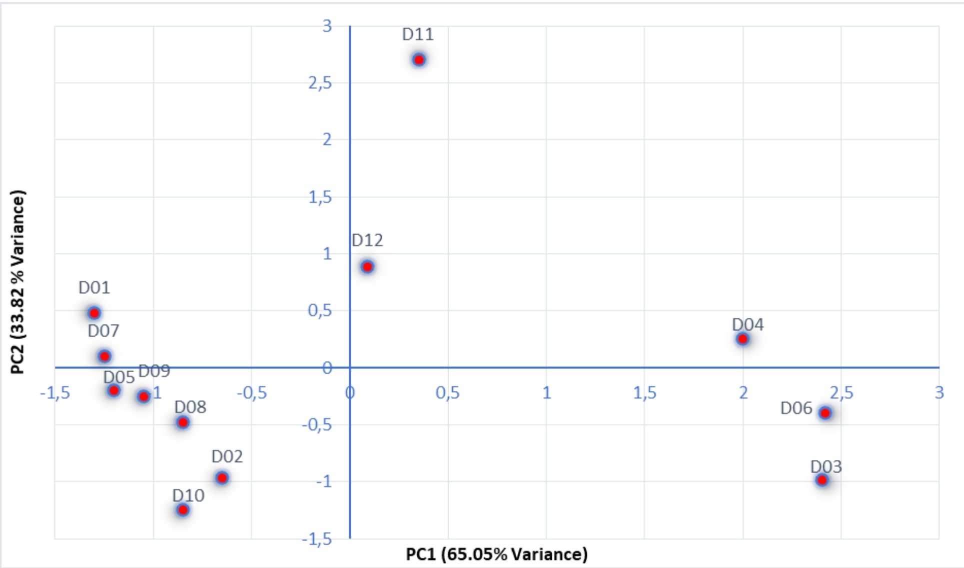

Figure 4: PCA of Radioactive Elements.

6 Radiological Hazards

Table 7 presents the (Ra_{eq}) values range and average 37.89 – 243.52 Bq/kg, 108.85 Bq/kg respectively, well below the safety value 370 Bq/kg (UNSCEAR, 2008). Similarly, the absorbed dose rate (DR) spans from 18.36 to 119.63nGy/h, with a mean of 52.1nGy/h. While most samples fall within the safe boundary of 55nGy/h suggested by UNSCEAR (UNSCEAR, 2000), some, such as D03, D04, and D06, exceed this threshold, indicating a potential for increased indoor radiation exposure.

The ($\mathrm{AEDE}_{\mathrm{indoor}}$) varies from 0.01 to 0.58mSv/y, with an average of 0.25mSv/y as in Tabel 7. Though the average is below the safety limit of 0.5mSv/y for the general public (ICRP, 1993), individual samples-particularly D03, D04, and D06-again exceed this value slightly, emphasizing the need for caution when these materials are used in enclosed spaces with high occupancy.

Hazard indices (H_{in} and H_{ex}) for all samples remain below the recommended limit of 1

(European Commission, 1999), with maximum values of 0.68 and 0.65 , respectively. This indicates that none of the studied materials poses an immediate hazard from the standpoint of internal or external exposure based solely on these indices.

However, the $\text{ELCR}_{\text{indoor}}$ values ranged from 0.31×10^{-3} to 2.03×10^{-3}, with an average of 0.90×10^{-3}. These average approaches the upper threshold of 1×10^{-3} recommended by international guidelines (UNSCEAR, 2000), and individual samples such as D03, D04, and D06 exceed this value. According to UNSCEAR and ICRP, such elevated ELCR values may correspond to a non-negligible increase in the probability of cancer development over a lifetime, particularly under long-term indoor exposure.

Furthermore, the AUI, which evaluates the material's suitability for bulk use in construction, ranged from 0.18 to 1.06 . While the majority of samples fall below the critical limit of 1 (UNSCEAR, 2008), three samples (D03, D04, D06) exceed this benchmark, suggesting restricted usage should be considered for these materials, especially in living spaces with limited ventilation.

These results are broadly consistent with previous Iraqi studies reporting safe levels for most building materials. For example, Essa et al. found Raeq of 40.45 Bq/kg and DR of 18.67nGy/h in cement samples (Essa et al., 2025), and Jassim and Abojassim reported Raeq of 65.0 ± 5.8 Bq/kg, DR of 31.3 ± 2.8nGy/h, and ELCR of $0.537 \times 10^{-3}-$ close to the present study's average (Jassim et al., 2022). Similarly, Amana et al. measured AEDE of 0.220mSv/y and ELCR of 0.771×10^{-3} in cement, slightly lower than our results (Amana et al., 2021).

Conversely, other works documented much higher hazard parameters. Ahmed reported DR values up to 200.9 ± 14nGy/h and Hin of 1.7 (Ahmed, 2005), while Pavlidou et al. recorded DR up to 364.8nGy/h and AEDE up to 1.5mSv/y in European granite (Pavlidou et al., 2006) - well above the maxima in this study ($\text{DR} = 119.63\text{nGy/h}, \text{AEDE} = 0.58\text{mSv/y}$). Nonetheless, our highest values (e.g., $\text{Raeq} \approx 243.52$ Bq/kg, $\text{DR} > 119.63\text{nGy/h}, \text{ELCR} > 1.8 \times 10^{-3}$ in D03, D04, D06) are comparable to those reported by AI-Zahrani in imported granite [Al-Zahrani (2017)] and overlap with the upper ranges documented by (Imani et al., 2021).

Table 7: Ra_{eq}, DR, AEDE indoor, H_{in}, H_{ex}, ELCR $_{indoor}$, and AUI for samples collected from Iraqi markets.

Samples	Ra_{eq}	DR	AEDE	H_{in}	H_{ex}	ELCR $\times 10^{-3}$	AUI
D01	39.21	19.30	0.01	0.15	0.11	0.32	0.21
D02	63.04	31.23	0.15	0.18	0.17	0.53	0.26
D03	232.67	113.17	0.55	0.63	0.62	1.92	1.06
D04	225.42	110.47	0.53	0.64	0.60	1.87	1.01
D05	39.89	19.34	0.01	0.14	0.10	0.33	0.22
D06	243.52	119.63	0.58	0.68	0.65	2.03	1.05
D07	37.89	18.36	0.09	0.14	0.10	0.31	0.22
D08	55.50	26.67	0.12	0.17	0.14	0.45	0.30
D09	47.50	23.37	0.11	0.16	0.12	0.39	0.23
D10	49.49	24.96	0.12	0.14	0.13	0.42	0.18
D11	155.14	73.85	0.35	0.51	0.41	1.25	0.90
D12	116.93	55.00	0.26	0.36	0.31	0.93	0.70
Min	37.89	18.36	0.01	0.14	0.10	0.31	0.18
Max	243.52	119.63	0.58	0.68	0.65	2.03	1.06
Mean	108.85	52.1	0.25	0.32	0.29	0.90	0.53
Safe limit	370	55	0.5	< 1	< 1	1.16	1
	UNSCEAR (2008)	UNSCEAR (2000)	ICRP (1993)	European Commission (1999)	European Commission (1999)	UNSCEAR (2000)	UNSCEAR (2008)

Overall, while the averages in this study fall within international safety guidelines, the presence of a few samples exceeding AEDE and ELCR thresholds suggests that certain decorative materials—especially those imported from specific countries-may pose a higher radiological risk and should be monitored accordingly.

7 Conclusion

The results showed that sample D11 exhibited a specific activity for ^{238}U higher than the UNSCEAR-recommended limit. Additionally, several samples recorded specific activities of ^{232}Th and ^{40}K that exceeded those limits. For instance, the highest ^{232}Th and ^{40}K values were found in samples associated with granites, suggesting that materials sourced from certain countries or quarries carry a higher radiological load. These variations underscore the need for targeted screening of high-risk imports rather than relying on average values alone. The elevated ^{40}K and ^{232}Th levels are likely attributable to the mineralogical composition and geochemical origin of the raw materials used, such as potassium- and thorium-rich rocks (e.g., granite or syenite). The statistical analysis indicated no significant correlation between ^{238}U and ^{232}Th or ^{238}U and ^{40}K. However, a strong positive correlation was observed between ^{232}Th and ^{40}K($r = 0.94$), which is consistent with their geochemical behavior as incompatible elements that concentrate in the residual melt during magmatic differentiation and co-occur in accessory minerals such as K-feldspar, muscovite, biotite, and monazite. Also, PCA analysis showed clear grouping of samples according to their radionuclide levels, indicating differences in geological origin.

These findings suggest that the origin of the raw materials plays a major role in the enrichment of natural radionuclides. Some natural rock types, especially two-mica granites, inherently contain high concentrations of ^{232}Th and ^{40}K due to prolonged geological accumulation. While the average radiological parameters across all samples remain below international safety thresholds set by UNSCEAR, a subset of the decorative materials-primarily imported granites and ceramics-exhibited radiological characteristics that could pose a health risk, especially in high-occupancy indoor settings. Therefore, the study highlights a crucial need for implementing national standards and radiological screening protocols for imported building and decorative materials, especially those with granitic origin.

Acknowledgement

The author thanks Prof. Dr. Abojassim, A.A., for their endless support in performing the practical part of this research in the Nuclear Physics Laboratory, College of Science, University of Kufa.

Competing Interests

The author affirms that no financial, personal, or professional interests could potentially influence, or be perceived to influence, the outcomes or interpretations of the research presented in this paper.

Funding Information

The author solely bore all costs related to this study, and no financial assistance was obtained from any external source.

References

Abdel-Hakeem, M., El-Tahir, M., Zeid, E. A., & Rageh, H. (2023). Genetic implications of Th/U, Th/K, and U/K ratios for U mineralizations: A case study from El-Missikat and El-Erediya shear zones, Eastern Desert, Egypt. *Geochemical Transactions*, *24*(1), 3.

Abdellah, W. M., Mansour, N. A., Diab, H. M., Hassan, N. M., Kasem, A., & Ibrahim, M. H. (2018). Evaluation of natural radioactivity and its radiation hazards in some building and decorative materials in Iraq. *Arab J. Nucl. Sci. Appl*, *51*(1), 39.

Ahmed, N. K. (2005). Measurement of natural radioactivity in building materials in Qena city, Upper Egypt. *Journal of Environmental Radioactivity*, *83*(1), 91–99.

Albaréde, F. (2003). *Geochemistry: An Introduction* (1st ed.). Cambridge University Press. ISBN: 978-0521891486

Alhous, S. F., Kadhim, S. A., Alkufi, A. A., Muhmood, A. A., & Zgair, I. A. (2020, November). Calculation of radioactivity levels for various soil samples of Karbala-Najaf road (Ya-Hussein)/Iraq. In *IOP Conference Series: Materials Science and Engineering*, *928*(7), p. 072076. IOP Publishing.

Ali, K. K. (2012). Radioactivity in building materials in Iraq. *Radiation Protection Dosimetry*, *148*(3), 372–379.

Ali, R. M., Gadhban, A. Q., Baqir, Y. A., & Alebadi, S. N. (2025). Evaluation of the natural radioactivity (^{238}U, ^{232}Th, ^{40}K) in building materials used in Iraqi homes. In *E3S Web of Conferences*, *633*, p. 08006. EDP Sciences. https://doi.org/10.1051/e3sconf/202563308006

Ali, Y. F., Cucinotta, F. A., Ning-Ang, L., & Zhou, G. (2020). Cancer risk of low dose ionizing radiation. *Frontiers in Physics*, *8*, 234.

Al-Sewaidan, H. A. (2019). Natural radioactivity measurements and dose rate assessment of selected ceramic and cement types used in Riyadh, Saudi Arabia. *Journal of King Saud University-Science*, *31*(4), 987–992.

Al-Zahrani, J. (2017). Estimation of Natural Radioactivity in Local and Imported Polished Granite Used as Building Materials in Saudi Arabia. *Journal of Radiation Research and Applied Sciences*, *10*(3), 241–245. https://doi.org/10.1016/j.jrras.2017.05.001

Amana, M. S. (2017). Radiation hazard index of common imported ceramic using for building materials in Iraq. *Australian Journal of Basic and Applied Sciences*, *11*(10), 94–102.

Amana, M. S., Jubier, N. J., Aldhuhaibat, M. J., & Salim, A. A. (2021). Assessment of radioactivity levels in some cement produced locally in Iraq. *Radiation Detection Technology and Methods*, *5*, 633–640.

Asgharizadeh, F., Abbasi, A., Hochaghani, O., & Gooya, E. S. (2012). Natural radioactivity in granite stones used as building materials in Iran. *Radiation Protection Dosimetry*, *149*(3), 321–326.

Aswood, M. S., Salih, A. A., & Al Musawi, M. S. A. (2019, July). Long-lived gamma-ray measurement in soil samples collected from city central of Al-Diwaniyah, Iraq. In *Journal of Physics: Conference Series*, *1234*(1), p. 012003. IOP Publishing.

Baha, A., Hashim, S., Sanusi, M. M., Chik, E. M. F. E., Hanifah, N. A., Hassan, H. J., & Zulkeplee, S. A. (2023). Radioactivity in decorative building materials: Insights from Johor, Malaysia. *Radiation Physics and Chemistry*, *209*, 111006.

Curtis, D. (1956). Selected annotated bibliography of the uranium geology of igneous and metamorphic rocks in the United States and territories (No. 534). https://pubs.usgs.gov/tei/534/report.pdf

Darwish, D. A. E., Abul-Nasr, K. T. M., & El-Khayatt, A. M. (2015). The assessment of natural radioactivity and its associated radiological hazards and dose parameters in granite samples from South Sinai, Egypt. *Journal of Radiation Research and Applied Sciences*, *8*(1), 17–25.

Dawal, A. A. A. H., & Oudah, O. N. (2025). Measurement of natural radioactivity and radiation hazards in bricks produced in Babylon brick factories, Iraq. *Radiation Protection Dosimetry*, *201*(4), 261–269.

Dos Santos Júnior, J. A., de Araújo, E. E. N., Fernández, Z. H., dos Santos Amaral, R., do Nascimento Santos, J. M., & Milán, M. O. (2021). Measurement of natural radioactivity and radium equivalent activity for pottery making clay samples in Paraíba and Rio Grande do Norte–Brazil. *Environmental Advances*, *6*, 100121.

Essa, S. A., Mohammad, K. K., & Mahmood, Y. H. (2025, April). Radionuclides activity concentration for selected cement samples in Iraqi market. In *AIP Conference Proceedings*, *3282*(1), p. 050032. AIP Publishing LLC.

European Commission. (1999). Radiological protection principles concerning the natural radioactivity of building materials. *Radiation Protection*, *112*, Brussels, European Commission.

Fall, M., Baratoux, D., Jessell, M., Ndiaye, P. M., Vanderhaeghe, O., Moyen, J. F., ... & Bonzi, W. M. E. (2020). The redistribution of thorium, uranium, potassium by magmatic and hydrothermal processes versus surface processes in the Saraya Batholith (Eastern Senegal): Insights from airborne radiometrics data and topographic roughness. *Journal of Geochemical Exploration*, *219*, 106633.

Farhan, A. O., Ahmed, A. M., & Farhan, S. S. (2022). Estimation of the radioactive elements in raw materials utilized in the ceramic industry, Anbar, Western Iraq. *The Iraqi Geological Journal*, *55*(1B), 113–120.

Gaafar, I., Cuney, M., & Abdel Gawad, A. (2014). Mineral Chemistry of Two-Mica Granite Rare Metals: Impact of Geophysics on the Distribution of Uranium Mineralization at El Sela Shear Zone, Egypt. *Open Journal of Geology*, *4*, 137–160. https://doi.org/10.4236/ojg.2014.44011

Gambo, N., Ramli, R. M., & Noor Azman, N. Z. (2025). Gamma activity concentration from building materials: Estimation of gamma absorption and indoor radon concentration in Katsina State, Nigeria. *PloS One*, *20*(3), e0318497.

Hassan, N. M., Mansour, N. A., & Fayez-Hassan, M. (2013). Evaluation of radionuclide concentrations and associated radiological hazard indexes in building materials used in Egypt. *Radiation Protection Dosimetry*, *157*(2), 214–220.

Hassan, N. M., Mansour, N. A., Fayez-Hassan, M., & Fares, S. (2017). Assessment of radiation hazards due to exposure to radionuclides in marble and ceramic commonly used as decorative building materials in Egypt. *Indoor and Built Environment*, *26*(3), 317–326.

IAEA, International Atomic Energy Agency. (1989). Measurement of radionuclides in food and the environment: A guidebook (Technical Reports Series No. 295), Vienna.

Imani, M., Adelikhah, M., Shahrokhi, A., Azimpour, G., Yadollahi, A., Kocsis, E., ... & Kovács, T. (2021). Natural radioactivity and radiological risks of common building materials used in Semnan Province dwellings, Iran. *Environmental Science and Pollution Research*, *28*, 41492–41503. https://doi.org/10.1007/s11356-021-13469-6

International Commission on Radiological Protection (ICRP). (2011). ICRP Draft Report TG81: Radiological Protection against Radon Exposure. *Annals of the ICRP*, Elsevier, ICRP ref 4829-9671-6554.

International Commission on Radiological Protection. (1993). ICRP publication 65. *Annals of the ICRP*, *23*(2). Oxford: Pergamon Press.

Jafir, A. O., Hussein, M. I., Nadir, I. A., Sabr, B. N., & Ahmed, A. H. (2024). Assessment of Radioactivity in Building Materials: Implications for Health in Kurdistan Region of Iraq. *Aaro-the Scientific Journal of Koya University*, *12*(2), 23–32.

Jassim, A. S., Abojassim, A. A. (2022). Assessment of Natural radioactivity and its Radiological Hazard in Some Decorative Materials in Iraq. *Nuclear Physics & Atomic Energy*, *23*(1).

Joel, E. S., Maxwell, O., Adewoyin, O. O., Ehi-Eromosele, C. O., Embong, Z., & Oyawoye, F. (2018). Assessment of natural radioactivity in various commercial tiles used for building purposes in Nigeria. *MethodsX*, *5*, 8–19.

Kadhim, T. M., Alkufi, A. A., & Alhous, S. F. (2020, November). Measurement of the natural radiological activity of soil samples of some general education schools in Al-Qadisiyah Governorate. In *IOP Conference Series: Materials Science and Engineering*, *928*(7), p. 072026. IOP Publishing.

Keser, R., Görür, F. K., Akçay, N., & Okumuşoğlu, N. T. (2011). Radionuclide concentration in tea, cabbage, orange, kiwi and soil and lifetime cancer risk due to gamma radioactivity in Rize, Turkey. *Journal of the Science of Food and Agriculture*, *91*(6), 987–991.

Kumar, E., Subramani, T., Li, P., & Karunanidhi, D. (2022). Quantification of health and environmental risks due to radionuclides in limestone mining regions of Ariyalur, South India. *Human and Ecological Risk Assessment: An International Journal*, *28*(2), 243–264.

Malaysia, S., & Aswood, M. S. (2020). Determination of the radiological risk from the natural radioactivity in irrigation at selected areas of Peninsular Malaysia. *Sains Malaysiana*, *49*(6), 1439–1450.

Ministry of Health, Iraqi Cancer Board. (2022). Cancer registry of Iraq annual report. Republic of Iraq. https://storage.moh.gov.iq/2024/03/31/2024_03_31_11983087032_3940351786864953.pdf

Najam, L. A., Tawfiq, N. F., & Kitah, F. H. (2013). Measurement of natural radioactivity in building materials used in Iraq. *Australian Journal of Basic and Applied Sciences*, *7*(1), 56–66.

Omogunloye, O. Y., Chetty, N., & Ilori, A. O. (2025). Assessment of natural radioactivity and associated radiological hazards in some building materials commonly used in Pietermaritzburg, South Africa. *Environmental Forensics*, 1–12. https://doi.org/10.1080/15275922.2025.2459398

Omron, A. M., & Salim, M. D. (2020, November). Assessment of radioactivity and radiological hazards in some flooring materials used in Karbala governorate, Iraq. In *IOP Conference Series: Materials Science and Engineering*, *928*(7), p. 072006. IOP Publishing.

Othman, H. Q., & Hussein, Z. A. (2025). Radiological impacts of natural radioactivity and heavy metal of building material factories in Sulaymaniyah Governorate, Iraq. *International Journal of Environmental Analytical Chemistry*, 1–24. https://doi.org/10.1080/03067319.2025.2474501

Othman, S. Q., Ahmed, A. H., & Mohammed, S. I. (2023). Natural radioactivity and radiological risk assessment due to building materials commonly used in Erbil city, Kurdistan region, Iraq. *Environmental Monitoring and Assessment*, *195*(1), 140.

Pavlidou, S., Koroneos, A., Papastefanou, C., Christofides, G., Stoulos, S., & Vavelides, M. (2006). Natural radioactivity of granites used as building materials. *Journal of Environmental Radioactivity*, *89*(1), 48–60.

Salman, J. E., & Hassan, N. M. (2024). Evolution of radionuclide concentration and the radiological hazards in building material: a review. *Journal of Taibah University for Science*, *18*(1), 2370588.

Taqi, A. H., Shaker, A. M., & Battawy, A. A. (2018). Natural radioactivity in building materials from Kirkuk city of Iraq. *Journal of Radiation and Nuclear Applications*, *3*(3), 199–203. https://doi.org/10.18576/jrna/030310

Turhan, S., Kurnaz, A., & Karataşlı, M. (2022). Evaluation of natural radioactivity levels and potential radiological hazards of common building materials utilized in Mediterranean region, Turkey. *Environmental Science and Pollution Research*, *29*(7), 10575–10584.

UNSCEAR, (2000). United Nations Scientific Committee on the Effects of Atomic Radiation, Sources and effects of ionizing radiation, Vol. 1 sources. New York: United Nations Publications.

UNSCEAR, (2008). United Nations Scientific Committee on the Effects of Atomic Radiation. Sources, effects and risks of ionizing radiation. Report to the general assembly with scientific annexes A and B. New York.

Wakeford, R. (2004). The cancer epidemiology of radiation. *Oncogene*, *23*(38), 6404–6428.

Yang, S., & Lin, T. (2021, October). Measurement of natural radioactivity in building decoration materials in Nan'an city. In *Journal of Physics: Conference Series*, *2021*(1), p. 012057. IOP Publishing.

Zlobina, A., Farkhutdinov, I., Carvalho, F. P., Wang, N., Korotchenko, T., Baranovskaya, N., & Farkhutdinov, A. (2022). Impact of environmental radiation on the incidence of cancer and birth defects in regions with high natural radioactivity. *International Journal of Environmental Research and Public Health*, *19*(14), 8643.